Frequency Division Multiplexed Multichannel High-Speed Fluorescence Confocal Microscope

Fei Wu,* Xueqian Zhang,† Joseph Y. Cheung,† Kebin Shi,* Zhiwen Liu,* Claire Luo,‡ Stuart Yin,* and Paul Ruffin§

*Department of Electrical Engineering, Pennsylvania State University, University Park, Pennsylvania; †Departments of Cellular and Molecular Physiology and Medicine, Pennsylvania State University College of Medicine, Hershey, Pennsylvania; ‡General Opto Solutions, LLC, State College, Pennsylvania; and §United States Army Aviation and Missile Command, Redstone Arsenal, Alabama

ABSTRACT In this article, we report a new type of fluorescence confocal microscope: frequency division multiplexed multichannel fluorescence confocal microscope, in which we encode the spatial location information into the frequency domain. In this microscope, the exciting laser beam is first split into multiple beams and each beam is modulated at a different frequency. These multiple beams are focused at different locations of the target to form multiple focal points, which further generate multiple fluorescent emission spots. The fluorescent emissions from different focal points are also modulated at different frequencies, because the exciting beams are modulated at different frequencies (or difference carrier frequency). Then, all the fluorescent emissions (modulated at different frequencies) are collected together and detected by a highly sensitive, large-dynamic-range photomultiplier tube. By demodulating the detected signal (i.e., via the Fourier transform), we can distinguish the fluorescent light emitted from the different locations by the corresponding carrier frequencies. The major advantage of this unique fluorescence confocal microscope is that it not only has a high sensitivity because of the use of photomultiplier tube but also can get multiple-point data simultaneously, which is crucial to study the dynamic behavior of many biological process. As an initial step, to verify the feasibility of the proposed multichannel confocal microscope, we have developed a two-channel confocal fluorescence microscope and applied it to study the dynamic behavior of the changes of the calcium ion concentration during the single cardiac myocyte contraction. Our preliminary experimental results demonstrated that we could indeed realize multichannel confocal fluorescence microscopy by utilizing the frequency division multiplexed microscope, which could become an effective tool to study the dynamic behavior of many biological processes.

INTRODUCTION

The confocal microscope has become an effective tool to obtain three-dimensional (3D) imaging over the scattering media. In the past several decades, several types of confocal microscopes have been developed (1–8). In biomedical applications, fluorescence confocal microscopy is most commonly used for detecting fluorescent labels. By having a confocal pinhole, the microscope is really efficient at rejecting out of focus fluorescent light so that a high signal-to-noise ratio (SNR) image can be obtained over the scattering biomedical media (e.g., a cell).

To study the fast dynamic biologic behavior (e.g., the cardiac myocyte contraction), it would be great if a fast-speed, multichannel fluorescence confocal microscope were available. Unfortunately, although several types of multichannel confocal microscopic techniques have been developed (3–8), it has been very difficult to directly apply these techniques to the fluorescence confocal microscope. For example, since the emission wavelength of fluorescent light is determined by the fluorescent label, which is independent of the wavelength of the incident exciting beam, the wavelength division multiplexing technique (3,5) cannot be applied. Another major challenge comes from the weak fluorescent signal. To effectively detect the weak fluorescent signal, a photomultiplier tube (PMT) is usually used. In general, a PMT is a single-pixel detector. However, many multiplexing techniques (such as a microlens and pinhole arrays (4)) require a highly sensitive imaging detector (i.e., an array of detectors). Note that although PMT arrays have very recently been used as the detection modules (e.g., LSM 510 META detection module (Zeiss, Stuttgart, Germany), they usually have a very limited number of pixels (e.g., 32). In addition, these PMT array-based detection modules are very expensive. On the other hand, the sensitivity of the charge-coupled device (CCD)-based imaging detector is limited by the imaging speed. At the same SNR level, the higher the sensitivity, the lower the speed will be. A commonly available CCD imaging detector used for this application has a frame rate of around 30 frames/s (i.e., the video rate), which is not fast enough to monitor many fast dynamics happening in cells. For instance, a long-standing problem in cardiac research is how to obtain the transient 3D distribution of calcium in a cardiac myocyte during excitation-contraction. This requires both high spatial and high temporal resolutions (lateral and axial resolution $\sim$200 nm and $\sim$100 nm, temporal resolution $<$1 ms) for tracking multiple fluorescence points.

To overcome the limitations of the existing confocal technology, in this article, we present a novel nonscanning

Submitted February 17, 2006, and accepted for publication June 14, 2006.

Address reprint requests to Stuart Yin, Dept. of Electrical Engineering, Pennsylvania State University, University Park, PA 16802. E-mail: sxy105@psu.edu.

0006-3495/06/09/2290/07 $2.00

doi: 10.1529/biophysj.106.083337

multipoint fluorescence confocal microscope via frequency division multiplexion, which not only has a high spatial resolution but also has an unparalleled temporal resolution (up to the ns range, only limited by the lifetime of the fluorophores and the response time of PMT). This technology can be applied to both the PMT and the PMT array-based detection modules. In both cases, it increases the effective number of pixels (i.e., the number of pixels in the PMT multiplies the number of the frequency division multiplexed channels) in the detection module. Thus, this frequency division multiplexed fluorescence confocal microscope will become a very effective tool to study the transient dynamics that happen in living cells.

WORKING PRINCIPLE OF AN FDM FLUORESENCE CONFOCAL MICROSCOPE

To illustrate the working principle of an FDM fluorescence confocal microscope, let us consider a two-channel FDM fluorescence confocal microscope, as shown in Fig. 1. The incident laser beam with an output wavelength of 488 nm emitted from a Coherent Innova 300 Argon ion laser (Coherent, Santa Clara, CA) is divided into two beams by a beam splitter (i.e., BS1, as illustrated in Fig. 1). The intensities of two beams are then individually modulated at different carrier frequencies: $\omega_1 = 2\pi f_1$ and$\omega_2 = 2\pi f_2$, respectively. The two beams are then recombined by another beam splitter (i.e., BS2). After passing through the BS3, these two modulated beams are further coupled into the back aperture of the objective lens (PlanApo, 60×, NA 1.4, Nikon, Tokyo, Japan) at slightly different angles by beam splitter 3. The two modulated Gaussian beams are focused at two different locations in the sample (or target) by the objective lens to form two focusing spots. The distance between the two focused points can be adjusted by tuning the relative angle between two incident beams, which can be realized by adjusting the reflection angles of mirrors M1 and M2. The fluorescence emission from the sample at two focusing spots is collected by the same objective lens and reflected to the detection system by BS3. To view the sample and the location of focusing spots, a fourth beam splitter (BS4) is added in the detection portion of the system. The reflected light from BS4 is viewed by a CCD imaging system. The transmitted light from BS4 first passes though a bandpass fluorescence filter, which blocks the exciting laser beams and only transmits the fluorescence light. The transmitted fluorescence light beams from two focusing spots are then focused into two single-mode (SM) optical fibers by two objective lenses, as illustrated in Fig. 2. One fiber corresponds to one spot. The SM fibers serve two functions. First, they are used as pinholes to filter out the out-of-focus light and to achieve confocal imaging (9,10). Second, they allow us to conveniently couple two light beams into a single PMT photodetector. Assume that the fluorescent light intensities as a function of time for two spots are $f_1(t)$ and $f_2(t)$, respectively. Due to the frequency modulations, the intensities at fiber 1 and fiber 2 are $f_1(t)\cos(\omega_1 t)$ and $f_2(t)\cos(\omega_2 t)$, respectively. Then, the intensity detected by the PMT is the summation of these two intensities. Mathematically, the signal detected by PMT, $s(t)$, can be written as

$$s(t) = f_1(t)\cos(\omega_1 t) + f_2(t)\cos(\omega_2 t). \quad (1)$$

The output from the PMT is sent to a data acquisition board, which converts the analog electric signal to a digital signal. The digital output from the data acquisition board is input to a microcomputer. The microcomputer processes the data by taking the Fourier transform of the detected signal, $s(t)$. In the frequency domain, Eq. 1 can be shown as

$$S(\omega) = F_1(\omega - \omega_1) + F_2(\omega - \omega_2), \quad (2)$$

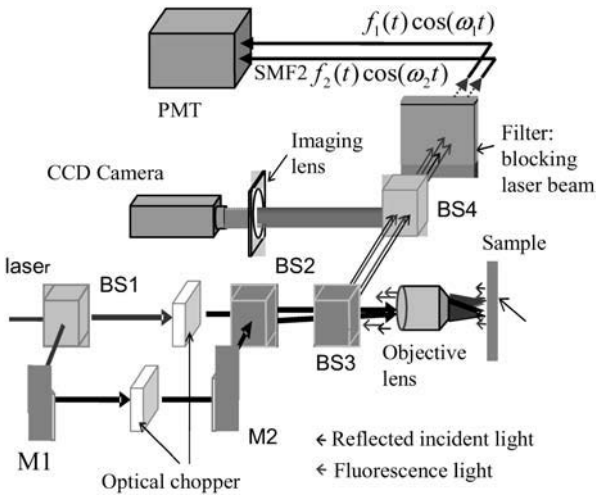

FIGURE 1 An illustration of a two-channel FDM fluorescence confocal microscope. *BS*, beam splitter; *M*, mirror.

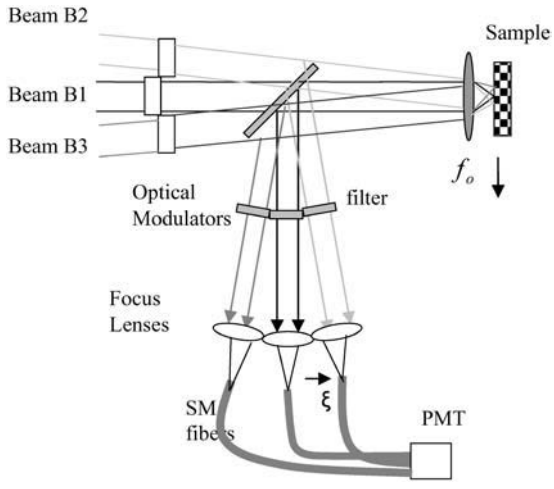

FIGURE 2 An illustration of multichannel confocal architecture using multiple optical fibers and a single PMT photodetector.

where $S(\omega), F_1(\omega)$, and $F_2(\omega)$ denote the Fourier transform of $s(t), f_1(t)$, and $f_2(t)$, respectively. As long as the carrier frequencies (i.e., ω_1 and ω_2) and their difference (i.e., $\omega_1 - \omega_2$) are larger than or equal to twice the highest signal frequency, there will be no overlap between two signals in the frequency domain, as illustrated in Fig. 3. Thus, one can easily separate two signals in the frequency domain by using the frequency bandpass filter. Note that it is not difficult to realize the required carrier frequency for this fluorescence confocal microscope application because one can modulate the light at very high speeds (e.g., up to GHz range), whereas most dynamic behaviors happening in the cell are in the millisecond range. Therefore, we can real-time detect and distinguish fluorescent emissions from multiple points by using a single-pixel, highly sensitive PMT, which offers the advantage of both high sensitivity and high speed.

The spatial resolution of this frequency-division multiplexed fluorescence confocal microscope is the same as that of the conventional fluorescence confocal microscope, as given by

$$\Delta r = 0.61\frac{\lambda}{NA} \quad \Delta z = 0.5\frac{\lambda}{NA^2}, \tag{3}$$

where Δr and Δz denote the lateral and axial spatial resolutions, respectively; λ is the fluorescent wavelength; and the NA represents the numerical aperture of the objective lens. Assuming that $\lambda = 0.5$ μm and NA $= 1.4$ (the parameters used in our experiments), the lateral and axial resolutions are around 0.2 μm and 0.1 μm, respectively, which are high enough for 3D imaging of a living cell.

EXPERIMENTAL SYSTEM DESCRIPTION

To verify the feasibility of the concept of the frequency division multiplexed multichannel confocal microscope, we set up a two-channel experimental demonstration system, which used the configuration illustrated in Fig. 1. An argon-ion laser with output wavelength 488 nm was used as the exciting light source. The two channels were modulated at 350 Hz and 400 Hz, respectively, by two optical choppers (that were conventionally used for lock-in amplifiers). A high-numerical-aperture objective lens (60X, NA 1.4, PlanApo, Nikon) was used as the focusing lens, which focused the two modulated beams on the sample.

In the experiment, a living rat cardiac myocyte that had a dimension of $\sim$100 μm in length and 20 μm in diameter was used as the sample. The fluo-4 AM ester dye (fluorescent calcium ion indicator, Invitrogen, Carlsbad, CA) was loaded in freshly isolated adult rat myocytes (1.8 μM, 30 min, at 37°C), which then emitted green light (520–540 nm) when they were illuminated by the 488-nm blue light. Fig. 4 shows the image when the two modulated laser beams focused on a living cardiac myocyte. The fluorescent emissions from these two spots were collected by the same focusing objective lens. A bandpass filter (520–540 nm) was used to block the exciting laser beam. The transmitted fluorescent emissions were coupled into two single-mode fibers by two objectives. A PMT (made by Hamamatsu) with a response time of $\sim$10 ns was used to detect these fluorescent emissions. If there was no noise, a beating sinusoidal signal (due to the summation of two different frequencies) would appear, as illustrated in Fig. 5, *a*. and *b*, shows the experimental signal output from the PMT. Due to the existence of the noise, the beating sinusoidal signal is not as nice as the curve shown in Fig. 5 *a*, but one can still see the beating between two sinusoidal waves. By taking the Fourier transform of Fig. 5 *b*, the fluorescence emission intensities from two spots can be determined by measuring the intensities of the frequency components at carrier frequencies, as shown in Fig. 6.

To monitor the transient dynamics, we can partition the measured fluorescence signal into many millisecond time windows. For each window, we can perform the Fourier transform and extract the fluorescence signal at the two different carrier frequencies (i.e., corresponding to two different locations). As a result, the transient dynamics at the two locations

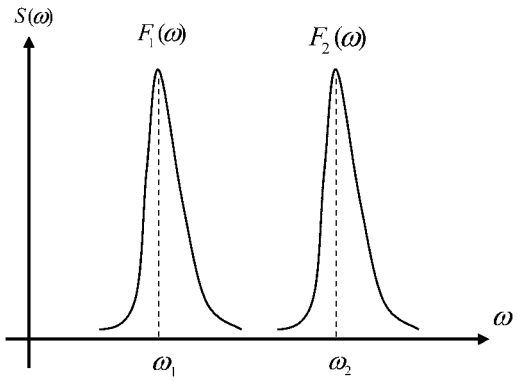

FIGURE 3 An illustration of signal separation in the frequency domain.

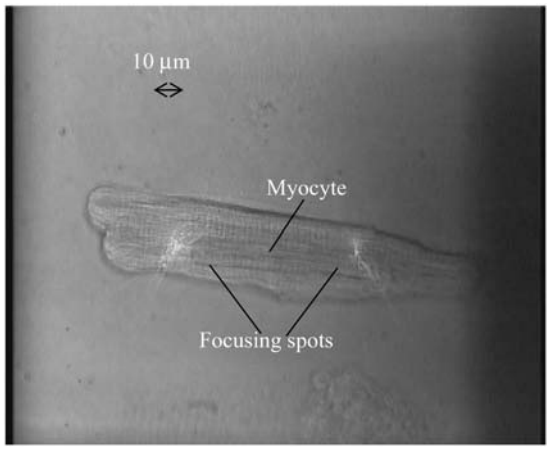

FIGURE 4 An image that shows a living rat cardiac myocyte and two focusing spots on the myocyte.

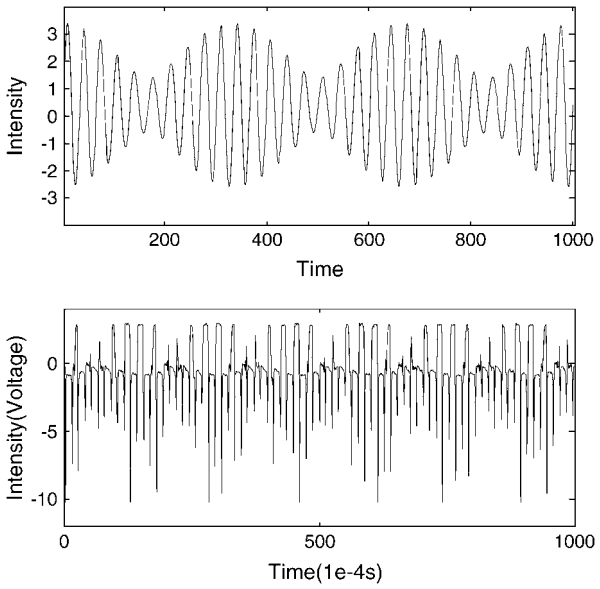

FIGURE 5 (*a*) Illustration of a simulated detected signal for two-channel FDM fluorescence confocal microscope without noise. (*b*). Detected signal by a PMT for two-channel FDM fluorescence confocal microscope with noise.

can be simultaneously obtained. This process is illustrated in Fig. 7.

APPLICATION OF FDM CONFOCAL MICROSCOPE TO STUDY THE SIMULTANEOUS CHANGES IN $[CA^{2+}]_{SM}$ AND $[CA^{2+}]_I$ IN A LIVING CARDIAC MYOCYTE

It is well known that Ca^{2+} occupies a central role in cardiac excitation-contraction coupling (11). During the contraction

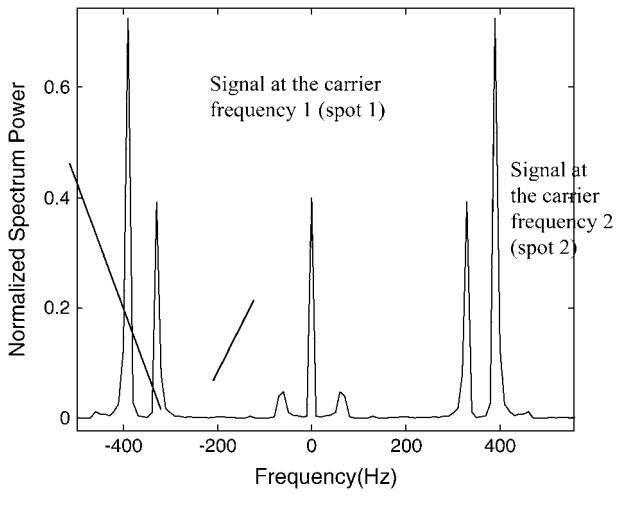

FIGURE 6 The detected signal by a PMT in the frequency domain. The fluorescent signal intensity of each spot can be determined by measuring the intensity of the frequency component at the corresponding carrier frequency.

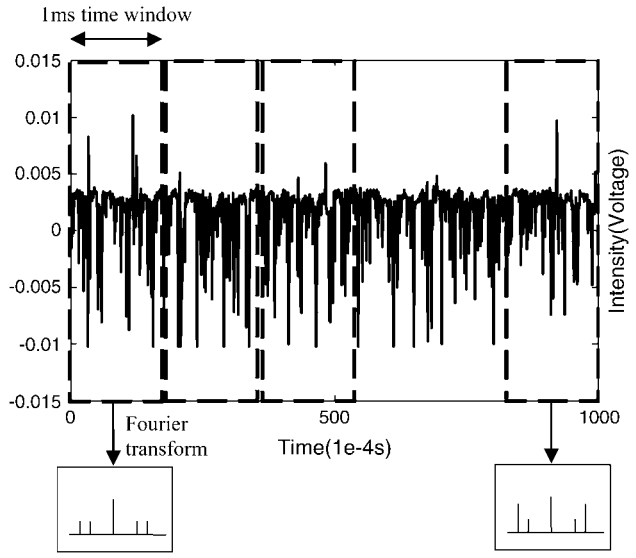

FIGURE 7 Schematic diagram illustrating the process to obtain the time dynamics from the detected fluorescence signal.

phase (systole), Na^+ channels open and the influx of extracellular Na^+ causes the membrane potential to become less negative. This membrane depolarization causes L-type Ca^{2+} channels to open, allowing extracellular Ca^{2+} to enter. A small amount of extracellular Ca^{2+} also enters via reverse Na^+/Ca^{2+} exchange (3 Na^+ out/1 Ca^{2+} in) (12). Entry of the small amount of extracellular Ca^{2+} triggers the release of stored Ca^{2+} in the sarcoplasmic reticulum (SR) to the myoplasm, resulting in a steep rise in cytosolic Ca^{2+} concentration ($[Ca^{2+}]_i$). Ca^{2+} then binds to troponin, resulting in myofilament activation and myocyte contraction. During the relaxation phase (diastole), most of the myoplasmic Ca^{2+} (70–92%) is resequestered in the SR by SR Ca^{2+}-ATPase, with a smaller amount of Ca^{2+} extruded by forward Na^+/Ca^{2+} exchange (3 Na^+ in: 1 Ca^{2+} out), and to a minor extent, by a separate Ca^{2+}-ATPase located in the plasma membrane (sarcolemma) of the myocyte. Thus, for each cardiac contraction-relaxation cycle, Ca^{2+} is cycled across the sarcolemma and SR membrane of the myocyte.

Recent high-resolution imaging suggests that the ion transporters involved in cardiac excitation-contraction coupling are grouped together to defined regions (*t*-tubules and triads) of the cardiac cell membrane (13). In addition, the cleft space between the L-type Ca^{2+} channel and the SR Ca^{2+} release channel (ryanodine receptor or RYR) is sufficiently small so that on opening of the Ca^{2+} channel, even though only a small amount of Ca^{2+} ions enter the cell, the local Ca^{2+} concentration in this ''cleft'' between the Ca^{2+} channel and RYR is likely to be substantially higher than that measured in the myoplasm. Other indirect evidence also suggests the existence of a ''submembranous'' domain in which the concentration of Ca^{2+} and Na^+ ions are significantly different than those in bulk myoplasm. Thus, the existence of a submembranous domain with ion concentrations significantly

different from those measured in bulk cytosol has major ramifications in terms of understanding the mechanisms of excitation-contraction coupling in the cardiac myocyte.

Despite the importance of answering the question of whether $[Ca^{2+}]_{sm}$ and $[Na^{+}]_{sm}$ do indeed exist in the cardiac myocyte or not, very few studies have provided direct measurements. Using electron microprobe x-ray analysis, $[Na^{+}]$ in rabbit papillary muscle was reported to be higher near the sarcolemma and fall to levels equal to that in bulk cytosol within 200–300 nm of the sarcolemma. It should be noted that electron microprobe x-ray analysis measures total, not free, ion concentrations and therefore the apparently increased $[Na^{+}]$ near the sarcolemma may reflect binding of Na in the subsarcolemmal space, which could in turn alter Na^{+} diffusion. In addition, the technique is necessarily destructive, and cannot be used to follow temporal changes in $[Ca^{2+}]_{sm}$ and $[Na^{+}]_{sm}$ in a living myocyte stimulated to contract.

To track simultaneous changes in $[Ca^{2+}]_{sm}$ and $[Ca^{2+}]_i$ in a living cardiac myocyte during an action potential, in this article, we applied our newly developed FDM fluorescence confocal microscope to simultaneously measure $[Ca^{2+}]_{sm}$ and bulk $[Ca^{2+}]_i$ in the same living cardiac myocyte.

Freshly isolated adult rat myocytes were loaded with fluo-4. The confocal laser excitation beams were directed separately onto the cell membrane region as well as the bulk cytosol. To ensure that one of the modulated laser excitation beams was localized at or near the cell membrane, and that the other was in the bulk cytosol, we ''doubly'' labeled the myocyte with a fluorescent membrane potential indicator (di-4-ANEPPS). Di-4-ANEPPS distributes to the charged plasma membrane (surface membranes and transverse tubules) with little to no signal in the cytosol. Because of the overlap between the emission spectrum of di-4-ANEPPS and fluo-4, a bandpass filter (520–540 nm) and a long-pass filter (550 nm) were applied separately to discriminate between the two emitted fluorescence signals.

Since fluo-4 is a single wavelength excitation fluorescent probe, its fluorescent intensity is proportional to the excitation light intensity, optical light path, fluorescent probe concentration, and free Ca^{2+} concentration. To ensure that the fluorescent intensity of fluo-4 reflects the free Ca^{2+} concentration in the region examined, first, the intensities of the two excitation beams were measured by measuring the intensities at two focusing spots and further balanced by adjusting the intensity of one of the beams until two beams had equal intensity. Second all the optical light paths were fixed. Finally, the uniformity of the concentration of fluo-4 was realized by following standard procedure (i.e., loading the fluo-4 at least 15 min at 37°C before doing the experiment (14)).

In the experiment, we first recorded the fluo-4 signal at rest, without applying the stimulating electric field. Then, we applied the stimulating electric field. To minimize the motion artifact of the myocyte when applying the stimulating electric field, we used cytochalasin D to immobilize the myocyte while preserving $[Ca]_i$ transients. We added diluted cytochalasin D (at the concentration level of 50 μmol/l) drop by drop at the amount of 1 μl per drop until the excitation-contraction of the cell was uncoupled. The myocyte was stimulated to contract by field electrodes at 1 Hz and the fluo-4 signals were continuously sampled and detected for 5–10 s. The detected data was processed according to the procedure as described in Sections 2 and 3. Fig. 8 shows the measured temporal variation of both the $[Ca^{2+}]_i$ around the membrane region and $[Ca^{2+}]_i$ in the bulk cytosol of the same myocyte concurrently by processing the recorded data. From this experimental result, we may draw the following conclusions first, the calcium ion concentration indeed changes during the cell contraction; second, the changing rate is the same as the exciting rate (i.e., 1 Hz, the beating behavior); and third, the calcium concentration at the submembranous region was around five to six times higher than that measured at the bulk cytosol region.

DISCUSSIONS

In this section, we would like to address some technical issues related to the proposed frequency division multiplexed fluorescence confocal microscope.

First, as shown in Figs. 3 and 6, the signal peaks have finite widths, which is mainly for the following two reasons. 1), The signals themselves have certain bandwidths. For example, for the rat cardiac cell contractions, the highest frequency components during the contraction processes are in the order of tens of Hz. 2), The existence of the noise can also contribute to the broadening of the bandwidths. The major noise source is the detector noise due to the weak

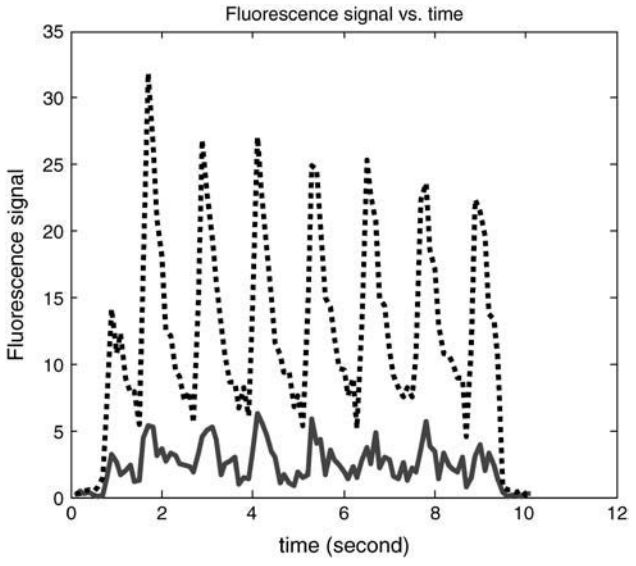

FIGURE 8 Detected intracellular Ca^{2+} concentration beating curves. *Solid curve*, fluorescence emission from the bulk region; *dashed curve*, fluorescence emission from the membrane region.

fluorescent signal. To minimize the detector noise-induced broadening effect, we want to make sure that the intensity of the detected fluorescent signal is within the linear region of the photodetector.

Second, we will discuss the cross-talk noise issue. The worst case scenario (i.e., the highest cross-talk case) happens when the two laser spots are focused in the same location. In this case, the signal separation can only be realized from the difference carrier frequency. Under the ideal case, without the noise, as long as the lowest carrier frequency and the separation between adjacent frequencies are twice the signal frequency (i.e., the Nyquist sampling theorem), there will be no cross talk among laser channels. However, due to the existence of the noise (e.g., the noise from the detector), there will be cross talk among different laser channels. Without losing the generality, assume that the noise is Gaussian noise. In this case, the bandwidth of the noise spectrum can be estimated by observing the detected signal over a finite time interval (15). Then, we will select the frequency and the frequency difference between adjacent channels at least twice this estimated spectral bandwidth, which will ensure a low cross-talk noise.

Third, we would like to estimate the maximum number of channels and the resolutions using this frequency division multiplexing approach. The spatial resolution of this method is similar to the conventional confocal microscope, as given by Eq. 3. Assuming that the numerical aperture of the objective lens is 1.4 and the operation wavelength is 0.5 μm, the lateral and depth resolutions are 0.2 μm and 0.1 μm, respectively. The temporal resolution of this method is determined by the response time of the fluorescent emission and the PMT photodetector, which is in the order of 10 ns. The maximum number of channels is limited by two factors: 1), response time of the fluorescent emission and the PMT photodetector; and 2), the dynamic range of the photodetector. Since 1-ms temporal resolution is usually fast enough to analyze the dynamic behavior of living cells, the response-time limited number of channels, M_r can be estimated by the following formula:

$$M_r = \frac{\text{signal temporal bandwidth}}{2 \times \text{temporal resolution}} = \frac{1\,\text{ms}}{2 \times 10\,\text{ns}} = 5 \times 10^4. \quad (4)$$

The dynamic-range limited number of channels may be estimated in the following way: Assume that the useful dynamic range of the PMT photodetector is 30 dB (i.e., 1000 in the linear scale, which is a realistic number) and the required dynamic range from each frequency channel is 10 dB (i.e., 10 in the linear scale). In this case, the dynamic-range limited number of channels, M_d is

$$M_d = \frac{\text{total dynamic range of the photodetector}}{\text{dynamic range of each channel}} = \frac{1000}{10} = 100. \quad (5)$$

Comparing Eq. 4 with Eq. 5, we know that the maximum number of channels is mainly determined by the dynamic range of the photodetector.

Finally, we would like to point out that the total number of channels can be further increased by employing a PMT array. Since a 32-channel PMT array is commercially available, by combining our frequency division multiplexing technique with the MPT array, the total number of channels can be as large as $100 \times 32 = 3200$, which is good enough for many confocal imaging applications.

CONCLUSIONS

We have developed a novel frequency division multiplexed multichannel fluorescence confocal microscope. The fluorescence emissions from different locations were modulated at different frequencies and detected by the same high-speed, highly sensitive photomultiplier tube. The location information was obtained by demodulating the detected signal via Fourier transform. This approach is similar to the frequency division multiplexed cable television system, in which multiple channels at different carrier frequencies are sent in a single cable and the channel selection is realized by choosing the proper carrier frequency. The major advantages of this unique fluorescence confocal microscope are: 1), the high speed, and 2), the high sensitivity. It could become an effective tool to study the transient dynamics happening within a cell. Although we only conducted a two-channel frequency division multiplexed confocal microscope experiment, this could readily be extended to multiplexing with more than two channels by slightly modifying the experimental set-up. Finally, we would like to point out that the experimental results of the application of this multiplexed confocal microscope to study the transient dynamics of calcium ion concentration during the cardiac myocyte contraction are very preliminary; this is mainly used to demonstrate the feasibility of this new type of confocal microscope. More thorough experimental study on transient calcium ion concentration will be conducted and reported in the future.

REFERENCES

1. Minsky, M. (19 Dec., 1962). Microscopy apparatus, U.S. Patent 3 013467.
2. Pawley, J. 1989. Handbook of Biological Confocal Microscopy. Plenum Press, New York.
3. Tearney, J., R. Webb, and B. Bouma. 1998. Spectrally encoded confocal microscopy. *Opt. Lett.* 23:1152–1154.
4. Fujita, K., O. Nakanura, T. Kaneko, M. Oyamada, T. Takamatsu, and S. Kawata. 2000. Confocal multipoint multiphoton excitation microscope with microlens and pinhole arrays. *Opt. Commun.* 174:7–12.
5. Yaqoob, Z., and N. Riza. 2002. Free-space wavelength-multiplexed optical scanner demonstration. *Appl. Opt.* 41:5568–5573.
6. Lin, C., and R. Webb. 2000. Fiber-coupled multiplexed confocal microscope. *Opt. Lett.* 24:954–956.
7. Blom, H., M. Johansson, M. Gosch, T. Sigmundsson, J. Holm, S. Hard, and R. Rigler. 2002. Parallel flow measurements in microstructures

by use of a multifocal 4 × 1 diffractive optical fan-out element. *Appl. Opt.* 41:6614–6620.

8. Carlsson, K., N. Aslund, K. Mossberg, and J. Philip. 1994. Simultaneous confocal recording of multiple fluorescent labels with improved channel separation. *J. Microsc.* 176:287–299.
9. Gu, M., C. Sheppard, and X. Gan. 1991. Image formation in a fiber-optical confocal scanning microscope. *J. Opt. Soc. Am. A.* 8:1755–1761.
10. Kimura, S., and T. Wilson. 1991. Confocal scanning optical microscope using single-mode fiber for signal detection. *Appl. Opt.* 30:2143–2150.
11. Bers, D. 2002. Cardiac excitation-contraction coupling. *Nature*. 415: 198–205.
12. Cheung, J., J. Song, L. Rothblum, and X. Zhang. 2004. Exercise training improves cardiac function postinfarction: Special emphasis on recent controversies on Na^{+}/Ca^{2+} exchanger. *Exerc. Sport Sci. Rev.* 32:83–89.
13. Scriven, D., P. Dan, and E. Moore. 2000. Distribution of proteins implicated in excitation-contraction coupling in rat ventricular myocytes. *Biophys. J.* 79:2682–2691.
14. Zhang, X.-Q., J. Song, L. I. Rothblum, M. Lun, X. Wang, F. Ding, J. Dunn, J. Lytton, P. J. McDermott, and J. Y. Cheung. 2001. Overexpression of Na+/Ca2+ exchanger alters contractility and SR Ca2+ contents in adult rat myocytes,. *Am. J. Physiol.* 281:H2079–H2088.
15. Proakis, J., C. Rader, F. Ling, and C. Nikias. Advanced Digital Signal Processing. Chapter 8. Power spectrum estimation, Macmillan, New York, 1992.